XVII. Ulusal Astronomi Kongresi VI. Ulusal Öğrenci Astronomi Kongresi
31 Ağustos - 4 Eylül 2010, Adana

X-ray Galaxies from Aquarius Supercluster

Mustafa Bozkurt[1⋆], Murat Hüdaverdi[2], Arzu Mert[1], Füsun Limboz[3], Metin Arık[1] and Akihiro Furuzawa[4]

[1] Boğaziçi University, Physics Department, 34342, Istanbul, Turkey
[2] TÜBİTAK Space Technologies Research Institute, METU Campus, 06531, Ankara, Turkey
[3] Istanbul University, Astronomy & Space Science Department, 34119, Istanbul, Turkey
[4] Nagoya University, Division of Particle & Astrophysical Science, 464-8602, Furu-cho, Chikusa, Nagoya, Japan

Özet We present the analysis results of ASCA and Chandra observations of 30 X-ray point sources from the Aquarius supercluster core. As being one of the highest concentrations of rich clusters, Aquarius offers an intense physical environment for galaxies. Here we focus on three of the clusters from the Aquarius central region: A2534, A2550, and A2556. All the detected pointed sources have optical counterparts (except 2 sources). The central bright galaxies are observed to be strong radio emitters. The X-ray spectral properties are studied and compared with field-galaxies. The enhanced X-ray emission from the sources is explained by ICM galaxy interaction in the high density cluster outskirts.

1 Introduction

Until the year 2000, Japanese satellite ASCA provided deep and sharp images of the X-ray sky. It allowed us, understand the ambiguous nature of X-ray emitting sources. For the last decade, Chandra's great sensitivity allows us to detect many X-ray emitters in the field besides the main target. In our recent projects of TÜBİTAK 109T092 and 108T0226 we aim to inspect cluster like structures and their mutual interactions in high-dense cosmic territories, namely superclusters of galaxies. Supercluster Candidate-100 (SCC100) also known as Aquarius, one of the intersection sites of the cosmic filaments in the nearby universe. About 10 clusters locate at Aquarius region. First systematic observations are performed by ASCA. Figure1 shows superposed mosaic images of GIS detector of ASCA in 0.5-2 keV soft energy band. In this work we have used high resolution Chandra ACIS data in order to study point like X-ray sources from the field. Three clusters (A2534, A2550, and A2556) from Aquarius core are analyzed for ACIS data. Heasoft 6.9 and xselect 2.4 version is used for cleaning and filtering of raw GIS detector event files. For Chandra data we used CIAO 4.2 version. In the following

⋆ mustafa.bozkurt@boun.edu.tr

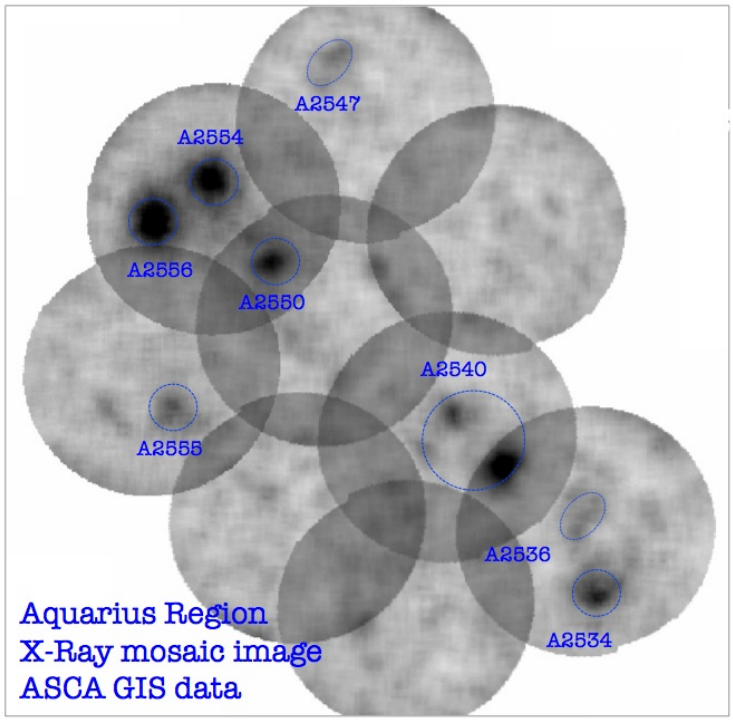

Şekil 1. ASCA mosaic image of Aquarius Supercluster.

sections, the physical properties of these sources is discussed. We assume a flat universe throughout the work.

2 Observations and Data Analysis

Aquarius supercluster region is well studied in optical band, but lack of complete results in X-rays. Thus, this work emphasizes X-ray properties of the region. Aquarius was systematically observed with ASCA around the year 2000. Here we have selected 3 observations with exposure >20ksec with GIS detector, because it has a larger field of view than SIS. Chandra observations of A2550, A2554 and A2556 are 59.8 ksec, 20.1 ksec and 20.1 ksec, respectively. Figure2 displays soft-band [0.3-8 keV] ACIS images of clusters. The wavdetect (CIAO) source detection algorithm is implemented to 0.3-8 keV band images. Considering the chip locations, variation in background level we have picked the points as X-ray AGNs with significance of 4σ. This selection criteria resulted 30 point like sources in total. Figure2 displays the location of the detected sources all over the ACIS chips. The difference of light sensitivity of BI (back-illuminated) and FI (front-

illuminated) chips are clearly evident from the images. The geometrical shapes and rotational angles are due to chip-gaps and viewing angle of ACIS detectors to the clusters. Spectral properties were further analyzed with XSPEC, version 12.6.0 software. The source counts were extracted within 30″ circular regions, and background counts are from 45″-60″ annular regions centered at the same X-ray peak. The response and ancillary files were created by *mkacisrmf* and *mkwarf* algorithm. The spectral properties were studied with single power-law model. The best fitted parameters are listed at the table below. The interstellar thermal and possible active nuclei properties are studied. The extracted counts are grouped into smaller bins (∼20 counts per channel) for definite spectral fit.

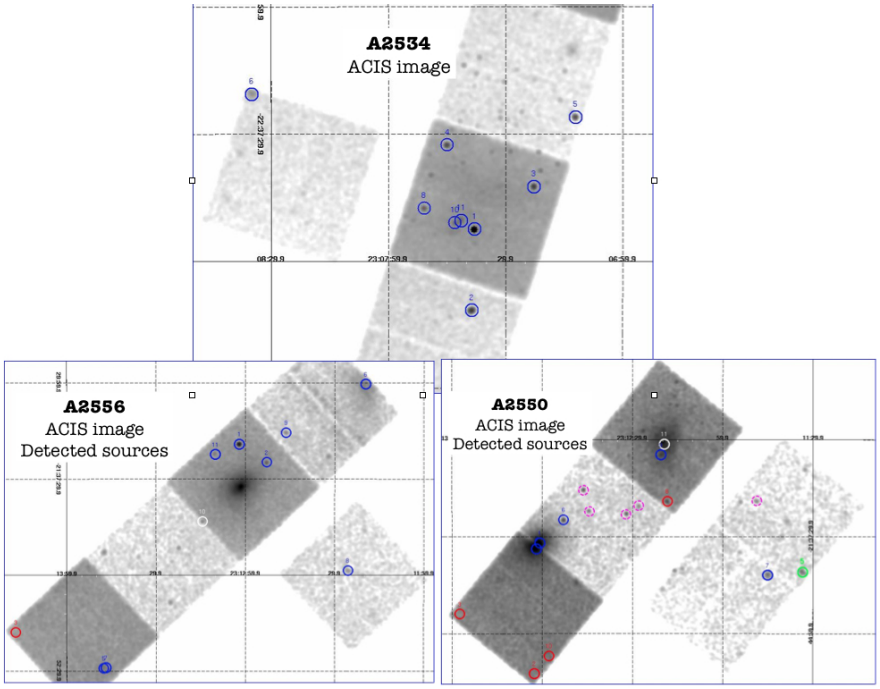

Şekil 2. Chandra - ACIS detector images of A2556, A2554, A2550 and the locations of the detected 30 point-like structures.

2.1 A2554 central region

In this section, we emphasize the spectral analysis results of A2554 central ACIS chip. These spectral properties are studied with meka+powerlaw model. Meka model is selected to describe interstellar thermal plasma. The power-law is representing the central emission from active nuclei. The best fit parameters and

90%error range values are listed at the Table4 below. Figure-3 shows the A2554 image, with spectra of two sources; #1 (cD galaxy) and #4 from ACIS chip corner. The binary #1 and #8 locate at the very center, #1 is bright in radio-band as it is seen in green in the figure-3. Considering F_X values, the source population seems to be a blend of LMXBs and AGNs. Our limited survey results suggest that active galaxies are crowded in cluster fields. The authors acknowledge the support of TÜBİTAK Scientific Projects #108T226 and #109T092. The readers are referred to proceeding ID#105 and ID#114 of this volume (Hudaverdi et al., 2010a, 2010b) for a detailed information about clusters and member galaxies.

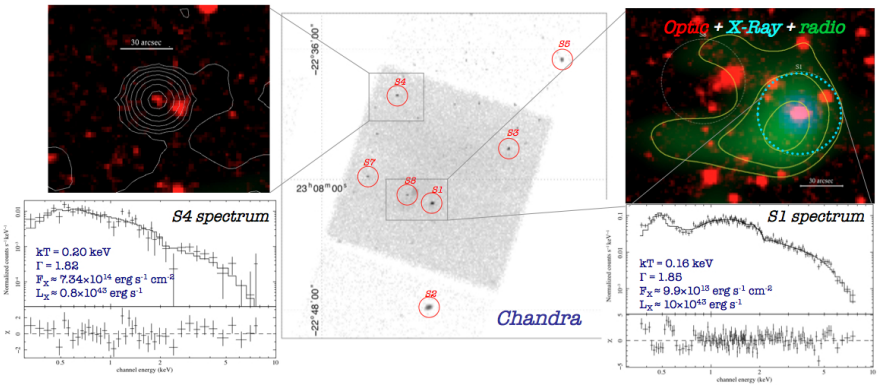

Şekil 3. J141649.4+522531 spectral fit of XMM-*Newton* (*left*) and Chandra (*right*)

	α (2000)	δ (2000)	redshift	kT_e(keV)	Photon Index	F_X(erg s^{-1} cm^{-2})	L_X(erg s^{-1})	χ^2/dof
S1	23:07:37.9	-22:43:05.76	0.191325	0.16±0.03	1.85±0.07	9.92 E-13	9.970×10^{43}	248/140 = 1.77
S2	23:07:38.6	-22:47:52.56	...	$0.18^{+0.99}_{-0.17}$	$1.85^{+0.20}_{-0.15}$	2.29 E-13	2.576×10^{43}	70/61 = 1.14
S3	23:07:22.7	-22:40:34.68	0.203577	$0.07^{+0.14}_{-0.04}$	$1.82^{+0.16}_{-0.11}$	7.23 E-14	0.839×10^{43}	58/50 = 1.16
S4	23:07:44.9	-22:38:08.42	...	$0.20^{+0.19}_{-0.13}$	$1.82^{+0.15}_{-0.13}$	7.34 E-14	0.793×10^{43}	147/149 = 0.99
S5	23:07:12.0	-22:36:28.77	no obj.	$0.03^{+0.04}_{-0.03}$	$2.01^{+0.32}_{-0.25}$	1.94 E-13	2.135×10^{43}	78/80 = 0.97
S6	23:08:34.9	-22:35:07.40	no obj.	0.5	$2.13^{+0.21}_{-0.19}$	1.12 E-13	1.236×10^{43}	24/27 = 0.88
S7	23:07:50.7	-22:41:51.36	...	...	$2.35^{+0.19}_{-0.04}$	1.01 E-14	0.124×10^{43}	26/26 = 1.01
S8	23:07:42.9	-22:42:43.02	0.203397	$0.84^{+0.66}_{-0.56}$	$2.14^{+0.19}_{-0.04}$	4.78 E-14	0.601×10^{43}	136/144 = 0.94

Şekil 4. The spectral best fit parameters of 8 sources from A2554.

Kaynaklar

Hudaverdi M, et al. 2010, Presentation ID#105, **UAK-2010** Proceeding Book
Hudaverdi M, et al. 2010, Presentation ID#114, **UAK-2010** Proceeding Book